Article

Tuning the Placement of Pt "Single Atoms" on a Mixed CeO_2–TiO_2 Support

Published as part of The Journal of Physical Chemistry virtual special issue "Cynthia Friend Festschrift".

Haodong Wang, Ning Rui, Sanjaya D. Senanayake, Lihua Zhang, Yuanyuan Li,* and Anatoly I. Frenkel*

ACCESS | Metrics & More | Article Recommendations | SI Supporting Information

ABSTRACT: Defect sites on the oxide supports can be used to anchor and activate "single-atom" catalysts (SACs). By engineering the anchoring sites for supporting SACs, one can alter their electronic and atomic structures which, in turn, define their activity, selectivity, and stability for catalytic reactions. To create and tune unique sites for Pt SACs on CeO_2 support, in this work, we synthesized a system consisting of CeO_2 decorated on TiO_2 nano-oxides for supporting the Pt SACs and investigated the effect of Pt weight loading. A combination of multiple structural characterization methods including diffuse reflectance infrared Fourier transform spectroscopy (DRIFTS), X-ray photoelectron spectroscopy (XPS), and X-ray absorption spectroscopy (XAS) was employed to characterize the distribution of charge states of single atoms and evaluate the heterogeneity of their binding sites. We have found that the placement of Pt atoms can be tuned on a mixed oxide surface by changing the weight loading of Pt.
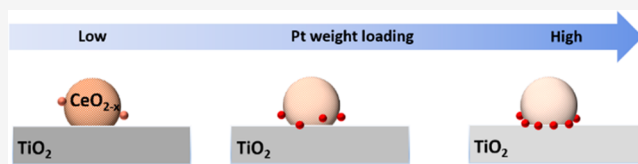
INTRODUCTION

"Single-atom" catalysts (SACs) have attracted tremendous attention due to their high atomic efficiency, activity, and selectivity for several chemical reactions[1−4] since the concept was developed by T. Zhang's group in 2011.[5] Nevertheless, their relative instability against sintering, especially in reducing reaction conditions, limits their applications.[6,7] Among many methods proposed to improve the stability of single atoms, the most commonly used one is to lower their weight loading to minimize the possibility of aggregation. The extremely low weight loadings of single atoms, however, will limit their use in industry and challenge the sensitivity of current characterization methods. Another approach to improve the stability of single atoms is to engineer the metal−support interaction.[8−11] So far, different oxide supports (Al_2O_3, Fe_2O_3, CeO_2, etc.) have been investigated for the purpose of increasing stability, activity, and selectivity of Pt SACs.[12−14] Among all the oxides, CeO_2 has been widely used due to its high reducibility and unique capability to localize atomically dispersed metal species.[15−18] Previously, we demonstrated that relatively high weight loading of Pt single atoms can be achieved by anchoring Pt single atoms on nanosized ceria.[19] Our other work also demonstrated that Pt single atoms on ceria support keep their atomically dispersed nature at higher reducing temperatures when Pt atoms are associated with oxygen vacancies.[20] The improved stability is due to the modified metal−support interaction and electronic properties of Pt single atoms, which will in turn affect their catalytic activity under reaction conditions.

While in our previous work we focused exclusively on the use of aliovalently doped ceria for creating defect sites for anchoring Pt SACs, the general questions about the role of defect sites and their manipulation for tuning the metal−support interaction of Pt SACs remain unanswered. We hypothesize that an opportunity to create, and rationally manipulate, the defect sites for anchoring Pt SACs on the oxide surface is by using mixed metal oxides. Here we report the test of this hypothesis by using CeO_2 nanoparticles that decorate TiO_2 as support for Pt SACs. Recent studies show that incorporating TiO_2 in addition to CeO_2 support could enhance the reducibility and oxygen mobility on CeO_2 support,[21,22] and unique sites could be formed at the interface of CeO_2–TiO_2.[23,24] In this work, a wet impregnation method was employed to deposit Pt on the surface of CeO_2 nanoparticles decorated TiO_2 support.[19,25,26] By using this type (mixed ceria−titania) of a catalytic support, due to the different binding energies of anchoring sites,[27,28] one would expect that Pt single atoms could be anchored on multiple sites: (1) on the surface of nanosized CeO_2, (2) at the interface between nanosized CeO_2 and TiO_2, or (3) at the surface of TiO_2, or in a combination of the possibilities 1 through 3 (Figure 1). We

found that the placement of Pt single atoms can be controlled by Pt weight loadings.
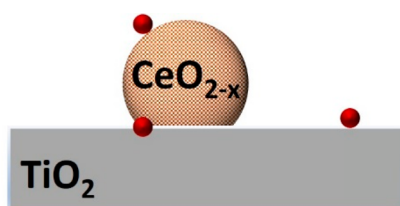

Figure 1. Schematic of possible anchoring sites of Pt single atoms on the nanosized CeO_2 decorated TiO_2 support.

To understand the complex environment of Pt SACs, we combined multiple structural characterization methods including diffuse reflectance infrared Fourier transform spectroscopy (DRIFTS), X-ray photoelectron spectroscopy (XPS), and X-ray absorption spectroscopy (XAS) to specifically investigate the placement of Pt single atoms as a function of Pt weight loading, characterize their charge states, and evaluate the heterogeneity of such sites.

EXPERIMENTAL SECTION

Sample Preparation. The samples were prepared following the previously described procedure.[19,25,26] All samples were prepared by dispersing 0.5 g of cerium(IV) oxide nanopowder (<25 nm) or titanium(IV) oxide nanopowder (<25 nm) in a solution of 0.42 g of cerium(III) nitrate hexahydrate, 2.0 g of urea, and 8 mL of water. The weight loading of Pt was controlled by adding the desired amount of Pt precursor solution (chloroplatinic acid hydrate in water, ~1 wt % Pt) in each system. All chemicals were purchased from Sigma-Aldrich. Ultrapure water was provided by a Millipore purification system. The mixture was sealed in a glass vial and stirred for 24 h in an oil bath at 90 °C. Afterward, the samples were washed by centrifuging in water three times. After drying overnight in an oven at 80 °C, the samples were crushed into powders and calcined at 500 °C (5 °C/min heating ramp) for 5 h. The resulting platinum loadings of all samples were measured by inductively coupled plasma optical emission spectrometry (ICP-OES) by Galbraith Laboratories. The instrument measures characteristic emission spectra by optical spectrometry and describes multielemental determinations.

Diffuse Reflectance Infrared Fourier Transform Spectroscopy (DRIFTS). The spectra were collected using an iS50 FTIR spectrometer equipped with a rapid-scanning liquid-nitrogen-cooled mercury cadmium telluride (MCT) detector and a Praying Mantis High Temperature Reaction Chamber (Harrick Scientific Products). Prior to measurement, each sample was heated at 150 °C for 30 min under He with a flow rate of 20 mL/min to remove surface adsorbed species. Afterward, the background spectrum was collected under He with a flow rate of 20 mL/min at room temperature. A mixture of 10% CO (balanced with He) with a flow rate of 20 mL/min flowed through the reaction chamber for 30 min to acquire CO adsorption spectra, followed by flowing with He with a flow rate of 20 mL/min for 30 min to acquire CO desorption spectra.

Ambient Pressure X-ray Photoelectron Spectroscopy (AP-XPS). The AP-XPS experiments were performed in a commercial SPECS AP-XPS chamber at the Chemistry Division of Brookhaven National Laboratory (BNL). A photon

energy of 1486.6 eV (Al $K\alpha$ source) was used to acquire the Ce 3d and Pt 4f spectra, which were recorded using a PHOIBOS 150 EP MCD-9 analyzer.

X-ray Absorption Spectroscopy (XAS). Pt L_3 edge XAS measurements were performed at the QAS beamline (7-BM) of National Synchrotron Light Source II (NSLS II), Brookhaven National Laboratory. All samples were prepared as pellets using a hydraulic press. For each sample, 30 scans were collected in fluorescence mode to increase the signal-to-noise ratio. The spectra were measured in ambient conditions (room temperature and pressure).

Electron Microscopy. Ex-situ electron microscopy was performed at the Center for Functional Nanomaterials at Brookhaven National Laboratory on a Hitachi 2700D scanning transmission electron microscope equipped with a probe aberration corrector operated at 200 kV.

RESULTS AND DISCUSSION

To study the Pt loading effects, we prepared three Pt/CeO_2-TiO_2 (PCT) samples: PCT(L), PCT(M), and PCT(H) with low, medium, and high Pt weight loading, respectively. For comparison, we also prepared Pt single atoms supported on CeO_2-CeO_2 using the same synthesis method. Similarly, the notations PCC(L) and PCC(H) are used for the $Pt-CeO_2-CeO_2$ samples. Table 1 provides a summary of Pt weight

Table 1. Summary of Pt Loadings

samples	weight loading (wt % Pt)	samples	weight loading (wt % Pt)
PCT(L)	0.60	PCC(L)	0.39
PCT(M)	2.93		
PCT(H)	4.37	PCC(H)	2.48

loadings in all samples obtained by ICP-OES elemental analysis. The structure of two representative samples was examined by scanning transmission electron microscopy, as shown in Figure S1.

In-situ CO-probe DRIFTS was employed to probe the surface distribution of Pt species in all samples. DRIFTS spectra for the three PCT samples are shown in Figure 2a. For comparison, the spectra for the two PCC samples are shown in Figure S2b. After CO desorption, a single narrow yet intense mode at 2091−2105 cm^{-1} is seen in all supported Pt samples, which can be assigned to CO bound atop isolated $Pt^{\delta+}$ sites.[17,29−31] The absence of the bridge bound CO on Pt (at ca. 1835 cm^{-1}) shown in Figure S2a also suggests that Pt atoms are singly dispersed in all samples. For PCT samples, with the increase of the Pt weight loading, the mode of the atop bound CO shifts to the higher wavenumbers, from 2091 to 2105 cm^{-1} (Figure 2a). Such a shift is not observed in PCC samples (Figure S2b), for which the peak for the atop bound CO shifts only slightly, from 2091 to 2093 cm^{-1}. For PCT(L) sample (Figure 2a), the peak for the atop bound CO is located at 2091 cm^{-1}, similar to that in PCC samples, suggesting therefore that in PCT(L) Pt single atoms reside on the surface of nanosized ceria support.[19] With the increase of the Pt weight loading, the peak shifts to 2100 cm^{-1} in PCT(M) and to 2105 cm^{-1} in PCT(H), i.e., toward the value characteristic of the Pt−CO vibration mode (2112 cm^{-1}) observed previously in the Pt/TiO_2 SACs system.[32]

There are two possible interpretations of these observations. First, they may be consistent with the gradual increase in the
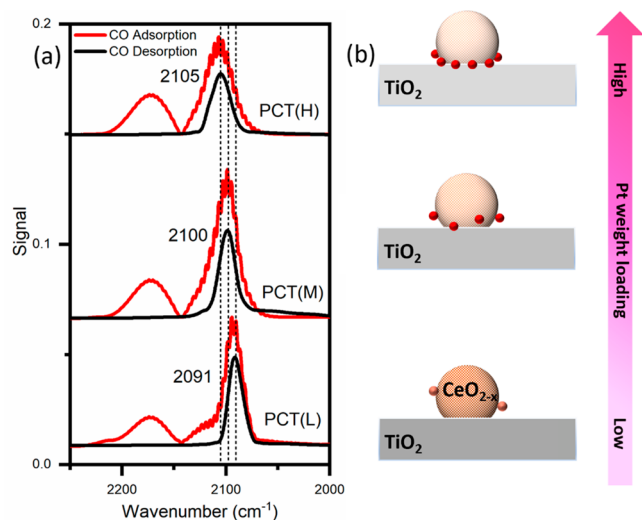
Figure 2. (a) DRIFTS spectra after CO adsorption (red) and CO desorption (black) of three PCT samples with different Pt loadings. (b) Schematic showing Pt placement on the CeO_2–TiO_2 support with increased Pt weight loading.

contribution of TiO_2-supported Pt SACs to the distribution of anchoring sites (that may include sites on both TiO_2 and nanosized CeO_2) with Pt weight loading increase. Such a change would result in the increased weight of the high wavenumber peaks to the ensemble-average spectrum and the shift of the overall atop bound CO mode to the higher wavenumbers compared to the spectrum for the lower weight loading, with predominant Pt–CeO_2 binding sites. This model is inherently heterogeneous and should be thus characterized by a broadening of the atop CO mode due to the coexistence of multiple inequivalent Pt sites. The second possibility, in which Pt single atoms remain on nanosized ceria but with a larger fraction on the ceria–titania interface (Figure 2b) as the Pt weight loading increases, would also require the atop bound CO mode to shift toward higher wavenumbers but remain narrow in all PCT samples due to the relative homogeneity of

Pt distributions (Pt atoms are not partitioned between ceria- and titania-supported populations, as in the first scenario). To discriminate between the two possible scenarios, both of which would result in the shifts of the atop CO mode to higher wavenumbers with Pt loading increase, we performed a control experiment. We physically mixed PCT(H) and PCC(H) samples, creating a bimodal distribution of Pt sites that gave rise to broad and multiple peaks that are clearly observed in Figure S2c. The observed coexistence of several adsorption features shown in this control experiment (Figure S2c) is in a striking contrast with a single narrow peak in PCT(M) and PCT(H) samples, consistent with homogeneous distribution of Pt near the CeO_2–TiO_2 interface in the PCT(M) and PCT(H) samples. Because the peak positions in these samples are between 2091 and 2112 cm^{-1}, Pt single atoms are likely located near/at the CeO_2–TiO_2 interface.

To obtain more information about the electronic properties and local coordination environment of Pt in different Pt single-atom sites, we performed XAS experiments. The Pt L_3 edge X-ray absorption near-edge structure (XANES) spectra for all PCT samples are shown in Figure 3a. The XANES spectra of the two PCC samples are shown in Figure S3a. The absence of visible changes between the PCC(L) and PCC(H) spectra is fully consistent with a weak contrast between their corresponding DRIFTS spectra (Figure S2b) discussed. EXAFS spectra of the PCC(H) sample in k-space and r-space are shown in Figures S3b and S3c, respectively. The spectra of Pt foil and α-PtO_2 are also included for comparison. The spectral features of PCT samples are quite different from that of Pt foil. Though the white line intensities of PCT samples are close to that of α-PtO_2, the resolved spectral features between 11580 and 11640 eV observed in the spectrum of α-PtO_2 are not observed in the spectra of PCT samples, suggesting that in PCT samples Pt has different local structures from that in α-PtO_2. As shown in the inset of Figure 3a, with the increase of the Pt weight loading, the white line decreases, suggesting Pt atoms at different sites have different bonding environments and/or electronic properties. Shifting the position from CeO_2 toward the interface with TiO_2 could
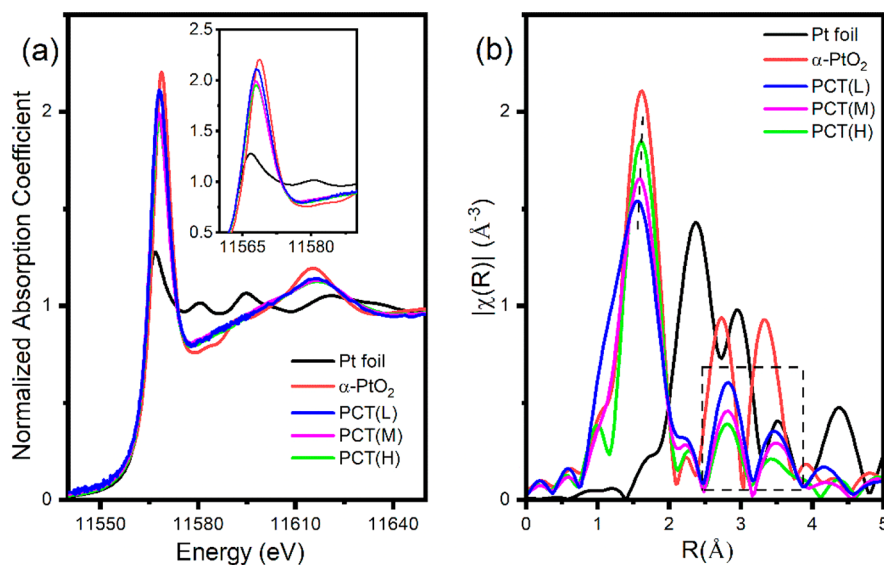

Figure 3. Pt L_3 edge XAFS spectra of three PCT samples. For comparison, the XAFS spectra of standards (Pt foil and α-PtO_2) are included. (a) XANES and (b) Fourier transform magnitudes of k^2-weighted EXAFS spectra.
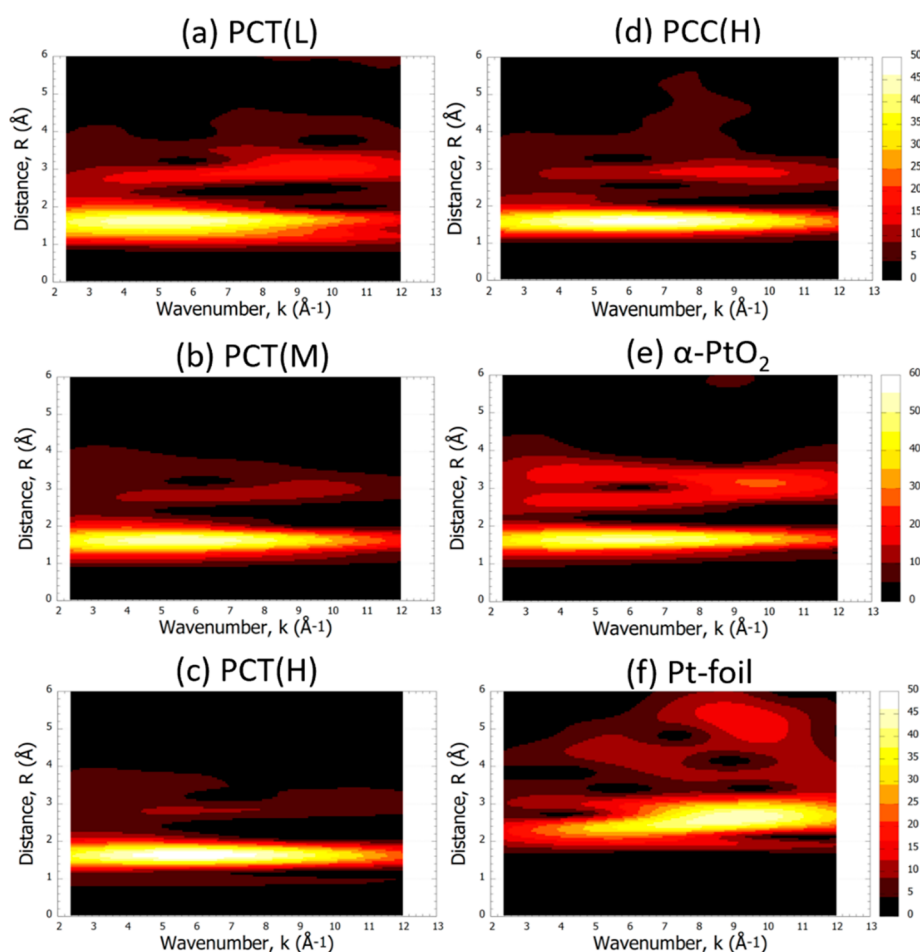
Figure 4. Wavelet transform (WT) EXAFS of (a) PCT(L), (b) PCT(M), (c) PCT(H), (d) PCC(H), (e) α-PtO$_2$, and (f) Pt foil.

result in the decrease of white line intensity.[33,34] Figure 3b shows the Fourier transform (FT) magnitudes of the extended X-ray absorption fine structure (EXAFS) data for PCT samples. The Pt−Pt contribution (between 2 and 3 Å) in the EXAFS spectrum of Pt foil is not observed in the spectra of PCT samples; hence, the formation of detectable Pt clusters/particles in PCT samples is not evident. For α-PtO$_2$, there are two peaks of comparable intensities between 2.5 and 4 Å. Though there are two peaks between 2.5 and 4 Å as well in PCT samples, the peak at about 2.7 Å is higher than that at about 3.5 Å, suggesting that in PCT samples Pt atoms have a different local binding environment from that in α-PtO$_2$. To obtain quantitative information about the local structure of Pt atoms, we performed EXAFS data analysis on the PCT(H) sample—the one that provided the relatively high quality of EXAFS data compared to the other two samples with lower loading. First, we performed EXAFS fitting on the α-PtO$_2$ reference and then used the same model to fit the PCT(H) sample. The fitting results shown in Figure S4b indicate that PtO$_2$ structure model does not provide a good fit for PCT(H) sample. Two other models give good agreement with experimental data and reasonable fitting results. Model 2 included Pt−O, Pt−Ce, and Pt−O scattering paths, while model 3 included Pt−O, Pt−Ti, and Pt−O scattering paths. The best fitting results are summarized in Table S1, and the comparison between the experimental and fitted spectra is plotted in Figure S4c,d. To further understand the Pt placement on support and metal−support interaction, an

additional tool for resolving between different possible structural and compositional motifs of the nearest environment of X-ray absorbing atoms is a wavelet transform (WT) EXAFS.[35−37]

The WT-EXAFS data show different regions in the $k-R$ map corresponding to the contributions of unique scattering species. As such, the WT-EXAFS is used as a fingerprinting method, capable of resolving between, e.g., metal−metal and metal−oxide pairs.[38] Indeed, as shown in WT-EXAFS maps (Figure 4), for PCT samples, the features between 2.5 and 4 Å are quite different from those of Pt foil and α-PtO$_2$, suggesting that for PCT samples the peaks observed between 2.5 and 4 Å in R space EXAFS (Figure 3b) are not due to the Pt−Pt contribution as in Pt foil or α-PtO$_2$. For PCT(L), the WT-EXAFS features are similar to those in PCC(H), suggesting that in these two samples Pt has similar local structure. In this structure, Pt coordinates with O and Ce at different bond distances.[19] With the increase of the Pt weight loading, the features between 2.5 and 4 Å in the WT-EXAFS map seem to shift the maxima to the lower wavenumber. The dependence of photoelectron scattering amplitudes for Pt−O, Pt−Ti, Pt−Ce, and Pt−Pt paths on wavenumber is shown in Figure S5. The contribution of Pt−Ti is centered at 5 Å^{-1}, in contrast with Pt−Ce which contributes strong intensity up to 12 Å^{-1}. This is in support of our hypothesis that in our PCT samples the local environment around Pt changes from CeO$_2$ rich to apparently TiO$_2$ rich, agreeing with DRIFTS results. Similar WT-EXAFS features were observed for Pt SACs on the TiO$_2$ support.[39]

Furthermore, the observations in WT-EXAFS confirm that the EXAFS fitting model which consists of Pt−O, Pt−Ti, and Pt−O contributions gives the best agreement with the experimental data of the PCT(H) sample.

By examining the XAFS data, we observed a seemingly conflicting trend. In XANES, the white line decreases with the increase of Pt loading, corresponding to decreasing the charge transfer from Pt single atoms to neighboring O atoms. However, in R space, as seen in Figure 3b, the expected decrease of first peak intensity with the increase of Pt loading which corresponds to Pt−O contribution was not observed. These results imply that the second-nearest-neighboring atoms (Ti or Ce) play a significant role here in redistributing electronic charge between Pt single atoms and the supports.[40] Therefore, the change in the nearest-neighboring environment from CeO_2 rich to TiO_2 rich affects not only the electronic properties of Pt single atoms but also the support. The effects of Pt weight loading on the properties of the support are also observed in the XPS data.

Figure 5 summarizes the distribution of Pt and Ce oxidation states in PCT samples as obtained by analysis of Pt 4f and Ce
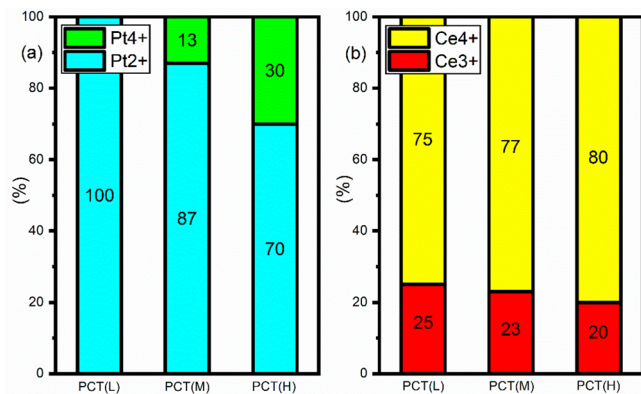

Figure 5. Distribution of Pt (a) and Ce (b) oxidation states by AP-XPS of three PCT samples with different Pt weight loadings.

3d XPS core level data. The data for two PCC samples are included in Figure S6. The raw spectra and peak fitting results for each sample are given in Figure S7. As shown in Figure 5, with the increase of Pt loading, there is an increase in the fraction of Pt^{4+}. The increase of Pt^{4+} fraction, however, did not lead to the increase in the Pt L_3 edge white line peak due to the influence from nearby Ti atoms (vide supra). In turn, with the increase of Pt loading, the fraction of Ce^{3+} (or associated O vacancies) decreases, offering fewer sites for Pt anchoring and facilitating the redistribution of Pt anchoring sites from CeO_2 toward the CeO_2−TiO_2 interface.[20,41−43] In contrast, the fraction of Ce^{3+} in PCC samples shows a small increase which indicates the more anchoring sites for Pt species. Combined with the DRIFTS and XAS results, XPS results further illustrate why Pt atoms show different preferred placements on CeO_2−TiO_2 and CeO_2−CeO_2 supports at increased weight loadings.

CONCLUSIONS

In this work, we found that the position of single atoms can be tuned on a mixed oxide surface by changing the weight loading of single atoms. As a result of the increase of the weight loading of Pt, a greater fraction of Pt atoms are located at the metal−support interface. As demonstrated in a Pt/CeO_2−TiO_2

system, the combined multiple techniques (DRIFTS, XAS, and XPS) suggest that Pt single atoms tend to homogeneously stay on the surface of nanosized CeO_2 at low Pt loading (0.6 wt %). When the Pt loading increases (up to 4.37 wt %), Pt atoms migrate toward the interface of the CeO_2−TiO_2 support while remaining relatively uniformly distributed. Our results suggest that the addition of Pt single atoms should affect the electronic properties of the support, leading to the redistribution and reconstruction of the anchoring sites. At different anchoring sites, due to the modified local bonding environment, the charge distribution between metal and support is different. Our study therefore provides a path for making SACs with tunable electronic properties, suitable for different catalytic reactions.

ASSOCIATED CONTENT

Supporting Information

The Supporting Information is available free of charge at https://pubs.acs.org/doi/10.1021/acs.jpcc.2c05198.

Electron microscopy images, additional DRIFTS results, XPS spectra, XAS spectra, and summary of EXAFS fitting results (PDF)

AUTHOR INFORMATION

Corresponding Authors

Yuanyuan Li − *Department of Materials Science and Chemical Engineering, Stony Brook University, Stony Brook, New York 11794, United States; Chemical Sciences Division, Oak Ridge National Laboratory, Oak Ridge, Tennessee 37831, United States;* orcid.org/0000-0003-3074-9672; Email: liy4@ornl.gov

Anatoly I. Frenkel − *Department of Materials Science and Chemical Engineering, Stony Brook University, Stony Brook, New York 11794, United States; Chemistry Division, Brookhaven National Laboratory, Upton, New York 11973, United States;* orcid.org/0000-0002-5451-1207; Email: anatoly.frenkel@stonybrook.edu

Authors

Haodong Wang − *Department of Materials Science and Chemical Engineering, Stony Brook University, Stony Brook, New York 11794, United States;* orcid.org/0000-0002-2344-2456

Ning Rui − *Chemistry Division, Brookhaven National Laboratory, Upton, New York 11973, United States;* orcid.org/0000-0001-6234-7075

Sanjaya D. Senanayake − *Chemistry Division, Brookhaven National Laboratory, Upton, New York 11973, United States;* orcid.org/0000-0003-3991-4232

Lihua Zhang − *Center for Functional Nanomaterials, Brookhaven National Laboratory, Upton, New York 11973, United States*

Complete contact information is available at:
https://pubs.acs.org/10.1021/acs.jpcc.2c05198

Notes

The authors declare no competing financial interest.

ACKNOWLEDGMENTS

■ REFERENCES

(1) Huang, P. P.; Huang, J. H.; Pantovich, S. A.; Carl, A. D.; Fenton, T. G.; Caputo, C. A.; Grimm, R. L.; Frenkel, A. I.; Li, G. H. Selective CO_2 Reduction Catalyzed by Single Cobalt Sites on Carbon Nitride under Visible-Light Irradiation. *J. Am. Chem. Soc.* **2018**, *140*, 16042−16047.

(2) Yan, H.; Cheng, H.; Yi, H.; Lin, Y.; Yao, T.; Wang, C. L.; Li, J. J.; Wei, S. Q.; Lu, J. L. Single-Atom Pd-1/Graphene Catalyst Achieved by Atomic Layer Deposition: Remarkable Performance in Selective Hydrogenation of 1,3-Butadiene. *J. Am. Chem. Soc.* **2015**, *137*, 10484−10487.

(3) Yang, X. F.; Wang, A. Q.; Qiao, B. T.; Li, J.; Liu, J. Y.; Zhang, T. Single-Atom Catalysts: A New Frontier in Heterogeneous Catalysis. *Acc. Chem. Res.* **2013**, *46*, 1740−1748.

(4) Chen, Z. P.; Vorobyeva, E.; Mitchell, S.; Fako, E.; Ortuno, M. A.; Lopez, N.; Collins, S. M.; Midgley, P. A.; Richard, S.; Vile, G.; et al. A Heterogeneous Single-Atom Palladium Catalyst Surpassing Homogeneous Systems for Suzuki Coupling. *Nat. Nanotechnol.* **2018**, *13*, 702−707.

(5) Qiao, B. T.; Wang, A. Q.; Yang, X. F.; Allard, L. F.; Jiang, Z.; Cui, Y. T.; Liu, J. Y.; Li, J.; Zhang, T. Single-Atom Catalysis of CO Oxidation Using Pt-1/FeO_x. *Nat. Chem.* **2011**, *3*, 634−641.

(6) Speck, F. D.; Paul, M. T. Y.; Ruiz-Zepeda, F.; Gatalo, M.; Kim, H.; Kwon, H. C.; Mayrhofer, K. J. J.; Choi, M.; Choi, C. H.; Hodnik, N.; et al. Atomistic Insights into the Stability of Pt Single-Atom Electrocatalysts. *J. Am. Chem. Soc.* **2020**, *142*, 15496−15504.

(7) Bruix, A.; Lykhach, Y.; Matolinova, I.; Neitzel, A.; Skala, T.; Tsud, N.; Vorokhta, M.; Stetsovych, V.; Sevcikova, K.; Myslivecek, J.; et al. Maximum Noble-Metal Efficiency in Catalytic Materials: Atomically Dispersed Surface Platinum. *Angew. Chem., Int. Ed.* **2014**, *53*, 10525−10530.

(8) Qiao, B. T.; Liang, J. X.; Wang, A. Q.; Xu, C. Q.; Li, J.; Zhang, T.; Liu, J. Y. Ultrastable Single-Atom Gold Catalysts with Strong Covalent Metal-Support Interaction (CMSI). *Nano Res.* **2015**, *8*, 2913−2924.

(9) Jiang, Z. Y.; Jing, M. Z.; Feng, X. B.; Xiong, J. C.; He, C.; Douthwaite, M.; Zheng, L. R.; Song, W. Y.; Liu, J.; Qu, Z. G. Stabilizing Platinum Atoms on CeO_2 Oxygen Vacancies by Metal-Support Interaction Induced Interface Distortion: Mechanism and Application. *Appl. Catal., B* **2020**, *278*, 119304.

(10) Li, J. J.; Guan, Q. Q.; Wu, H.; Liu, W.; Lin, Y.; Sun, Z. H.; Ye, X. X.; Zheng, X. S.; Pan, H. B.; Zhu, J. F.; et al. Highly Active and Stable Metal Single-Atom Catalysts Achieved by Strong Electronic Metal-Support Interactions. *J. Am. Chem. Soc.* **2019**, *141*, 14515−14519.

(11) Zhang, Q.; Qin, X. X.; Duan-Mu, F. P.; Ji, H. M.; Shen, Z. R.; Han, X. P.; Hu, W. B. Isolated Platinum Atoms Stabilized by Amorphous Tungstenic Acid: Metal-Support Interaction for Synergistic Oxygen Activation. *Angew. Chem., Int. Ed.* **2018**, *57*, 9351−9356.

(12) Kwon, H. C.; Park, Y.; Park, J. Y.; Ryoo, R.; Shin, H.; Choi, M. Catalytic Interplay of Ga, Pt, and Ce on the Alumina Surface Enabling High Activity, Selectivity, and Stability in Propane Dehydrogenation. *ACS Catal.* **2021**, *11*, 10767−10777.

(13) Duan, S. B.; Wang, R. M.; Liu, J. Y. Stability Investigation of a High Number Density Pt-1/Fe_2O_3 Single-Atom Catalyst under Different Gas Environments by HAADF-STEM. *Nanotechnology* **2018**, *29*, 204002.

(14) Jiang, D.; Yao, Y. G.; Li, T. Y.; Wan, G.; Pereira-Hernandez, X. I.; Lu, Y. B.; Tian, J. S.; Khivantsev, K.; Engelhard, M. H.; Sun, C. J.; et al. Tailoring the Local Environment of Platinum in Single-Atom Pt-1/CeO_2 Catalysts for Robust Low-Temperature CO Oxidation. *Angew. Chem., Int. Ed.* **2021**, *60*, 26054−26062.

(15) Li, Y. Y.; Kottwitz, M.; Vincent, J. L.; Enright, M. J.; Liu, Z. Y.; Zhang, L. H.; Huang, J. H.; Senanayake, S. D.; Yang, W. C. D.; Crozier, P. A.; et al. Dynamic Structure of Active Sites in Ceria-Supported Pt Catalysts for the Water Gas Shift Reaction. *Nat. Commun.* **2021**, *12*, 1−9.

(16) Montini, T.; Melchionna, M.; Monai, M.; Fornasiero, P. Fundamentals and Catalytic Applications of CeO_2-Based Materials. *Chem. Rev.* **2016**, *116*, 5987−6041.

(17) Nie, L.; Mei, D. H.; Xiong, H. F.; Peng, B.; Ren, Z. B.; Hernandez, X. I. P.; DeLariva, A.; Wang, M.; Engelhard, M. H.; Kovarik, L.; et al. Activation of Surface Lattice Oxygen in Single-Atom Pt/CeO_2 for Low-Temperature CO Oxidation. *Science* **2017**, *358*, 1419−1423.

(18) Cao, K.; Zoberbier, T.; Biskupek, J.; Botos, A.; McSweeney, R. L.; Kurtoglu, A.; Stoppiello, C. T.; Markevich, A. V.; Besley, E.; Chamberlain, T. W.; Kaiser, U.; Khlobystov, A. N. Comparison of Atomic Scale Dynamics for the Middle and Late Transition Metal Nanocatalysts. *Nat. Commun.* **2018**, *9*, 1−10.

(19) Kottwitz, M.; Li, Y.; Palomino, R. M.; Liu, Z.; Wang, G.; Wu, Q.; Huang, J.; Timoshenko, J.; Senanayake, S. D.; Balasubramanian, M.; Lu, D.; Nuzzo, R. G.; Frenkel, A. I. Local Structure and Electronic State of Atomically Dispersed Pt Supported on Nanosized CeO_2. *ACS Catal.* **2019**, *9*, 8738−8748.

(20) Wang, H. D.; Kottwitz, M.; Rui, N.; Senanayake, S. D.; Marinkovic, N.; Li, Y. Y.; Nuzzo, R. G.; Frenkel, A. I. Aliovalent Doping of CeO_2 Improves the Stability of Atomically Dispersed Pt. *ACS Appl. Mater. Interfaces* **2021**, *13*, 52736−52742.

(21) Chen, C. S.; Chen, T. C.; Wu, H. C.; Wu, J. H.; Lee, J. F. The Influence of Ceria on Cu/TiO_2 Catalysts to Produce Abundant Oxygen Vacancies and Induce Highly Efficient CO Oxidation. *Catal. Sci. Technol.* **2020**, *10*, 4271−4281.

(22) Vuong, T. H.; Radnik, J.; Rabeah, J.; Bentrup, U.; Schneider, M.; Atia, H.; Armbruster, U.; Grunert, W.; Bruckner, A. Efficient VO_x/Ce_{1-x}Ti_xO_2 Catalysts for Low-Temperature NH_3-SCR: Reaction Mechanism and Active Sites Assessed by in situ/Operando Spectroscopy. *ACS Catal.* **2017**, *7*, 1693−1705.

(23) Li, S. N.; Zhu, H. Q.; Qin, Z. F.; Wang, G. F.; Zhang, Y. G.; Wu, Z. W.; Li, Z. K.; Chen, G.; Dong, W. W.; Wu, Z. H.; et al. Morphologic Effects of Nano CeO_2-TiO_2 on the Performance of Au/CeO_2-TiO_2 Catalysts in Low-Temperature CO Oxidation. *Appl. Catal., B* **2014**, *144*, 498−506.

(24) Mosrati, J.; Abdel-Mageed, A. M.; Vuong, T. H.; Grauke, R.; Bartling, S.; Rockstroh, N.; Atia, H.; Armbruster, U.; Wohlrab, S.; Rabeah, J.; et al. Tiny Species with Big Impact: High Activity of Cu Single Atoms on CeO_2-TiO_2 Deciphered by Operando Spectroscopy. *ACS Catal.* **2021**, *11*, 10933−10949.

(25) Jeong, D. W.; Jang, W. J.; Shim, J. O.; Han, W. B.; Kim, H. M.; Lee, Y. L.; Bae, J. W.; Roh, H. S. Optimization of a Highly Active

Nano-Sized Pt/CeO₂ Catalyst via Ce(OH)CO₃ for the Water-Gas Shift Reaction. *Renewable Energy* **2015**, *79*, 78−84.

(26) Chen, Y.; Qiu, C. J.; Chen, C. L.; Fan, X. F.; Xu, S. B.; Guo, W. W.; Wang, Z. C. Facile Synthesis of Ceria Nanospheres by Ce(OH)CO₃ Precursors. *Mater. Lett.* **2014**, *122*, 90−93.

(27) Maslakov, K. I.; Teterin, Y. A.; Ryzhkov, M. V.; Popel, A. J.; Teterin, A. Y.; Ivanov, K. E.; Kalmykov, S. N.; Petrov, V. G.; Petrov, P. K.; Farnan, I. The Electronic Structure and the Nature of the Chemical Bond in CeO₂. *Phys. Chem. Chem. Phys.* **2018**, *20*, 16167−16175.

(28) Li, J.; Liu, Z.; Cullen, D. A.; Hu, W.; Huang, J.; Yao, L.; Peng, Z.; Liao, P.; Wang, R. Distribution and Valence State of Ru Species on CeO₂ Supports: Support Shape Effect and Its Influence on CO Oxidation. *ACS Catal.* **2019**, *9*, 11088−11103.

(29) Bazin, P.; Saur, O.; Lavalley, J. C.; Daturi, M.; Blanchard, G. FT-IR study of CO adsorption on Pt/CeO₂: Characterisation and Structural Rearrangement of Small Pt Particles. *Phys. Chem. Chem. Phys.* **2005**, *7*, 187−194.

(30) Xie, P. F.; Pu, T. C.; Nie, A. M.; Hwang, S.; Purdy, S. C.; Yu, W. J.; Su, D.; Miller, J. T.; Wang, C. Nanoceria-Supported Single-Atom Platinum Catalysts for Direct Methane Conversion. *ACS Catal.* **2018**, *8*, 4044−4048.

(31) Happel, M.; Myslivecek, J.; Johanek, V.; Dvorak, F.; Stetsovych, O.; Lykhach, Y.; Matolin, V.; Libuda, J. Adsorption Sites, Metal-Support Interactions, and Oxygen Spillover Identified by Vibrational Spectroscopy of Adsorbed CO: A Model Study on Pt/ceria Catalysts. *J. Catal.* **2012**, *289*, 118−126.

(32) DeRita, L.; Dai, S.; Lopez-Zepeda, K.; Pham, N.; Graham, G. W.; Pan, X. Q.; Christopher, P. Catalyst Architecture for Stable Single Atom Dispersion Enables Site-Specific Spectroscopic and Reactivity Measurements of CO Adsorbed to Pt Atoms, Oxidized Pt Clusters, and Metallic Pt Clusters on TiO₂. *J. Am. Chem. Soc.* **2017**, *139*, 14150−14165.

(33) Chen, L. X.; Unocic, R. R.; Hoffman, A. S.; Hong, J. Y.; Braga, A. H.; Bao, Z. H.; Bare, S. R.; Szanyi, J. Unlocking the Catalytic Potential of TiO₂-Supported Pt Single Atoms for the Reverse Water-Gas Shift Reaction by Altering Their Chemical Environment. *JACS Au* **2021**, *1*, 977−986.

(34) Jeantelot, G.; Qureshi, M.; Harb, M.; Ould-Chikh, S.; Anjum, D. H.; Abou-Hamad, E.; Aguilar-Tapia, A.; Hazemann, J. L.; Takanabe, K.; Basset, J. M. TiO₂-Supported Pt Single Atoms by Surface Organometallic Chemistry for Photocatalytic Hydrogen Evolution. *Phys. Chem. Chem. Phys.* **2019**, *21*, 24429−24440.

(35) Kottwitz, M.; Li, Y.; Wang, H.; Frenkel, A. I.; Nuzzo, R. G. Single Atom Catalysts: A Review of Characterization Methods. *Chemistry-Methods* **2021**, *1*, 278−294.

(36) Zhang, T. J.; Chen, Z. Y.; Walsh, A. G.; Li, Y.; Zhang, P. Single-Atom Catalysts Supported by Crystalline Porous Materials: Views from the Inside. *Adv. Mater.* **2020**, *32*, 2002910.

(37) Fang, S.; Zhu, X.; Liu, X.; Gu, J.; Liu, W.; Wang, D.; Zhang, W.; Lin, Y.; Lu, J.; Wei, S.; Li, Y.; Yao, T. Uncovering Near-Free Platinum Single-Atom Dynamics during Electrochemical Hydrogen Evolution Reaction. *Nat. Commun.* **2020**, *11*, 1−8.

(38) Huang, D. H.; de Vera, G. A.; Chu, C. H.; Zhu, Q. H.; Stavitski, E.; Mao, J.; Xin, H. L.; Spies, J. A.; Schmuttenmaer, C. A.; Niu, J. F.; et al. Single-Atom Pt Catalyst for Effective C-F Bond Activation via Hydrodefluorination. *ACS Catal.* **2018**, *8*, 9353−9358.

(39) Chen, L.; Unocic, R. R.; Hoffman, A. S.; Hong, J.; Braga, A. H.; Bao, Z.; Bare, S. R.; Szanyi, J. Unlocking the Catalytic Potential of TiO₂-Supported Pt Single Atoms for the Reverse Water-Gas Shift Reaction by Altering Their Chemical Environment. *JACS Au* **2021**, *1*, 977−986.

(40) O'Connor, N. J.; Jonayat, A. S. M.; Janik, M. J.; Senftle, T. P. Interaction Trends between Single Metal Atoms and Oxide Supports Identified with Density Functional Theory and Statistical Learning. *Nat. Catal.* **2018**, *1*, 531−539.

(41) Zhang, Q. S.; Bu, J. H.; Wang, J. D.; Sun, C. Y.; Zhao, D. Y.; Sheng, G. Z.; Xie, X. W.; Sun, M.; Yu, L. Highly Efficient Hydrogenation of Nitrobenzene to Aniline over Pt/CeO₂ Catalysts:

The Shape Effect of the Support and Key Role of Additional Ce3+ Sites. *ACS Catal.* **2020**, *10*, 10350−10363.

(42) Artiglia, L.; Orlando, F.; Roy, K.; Kopelent, R.; Safonova, O.; Nachtegaal, M.; Huthwelker, T.; van Bokhoven, J. A. Introducing Time Resolution to Detect Ce3+ Catalytically Active Sites at the Pt/CeO₂ Interface through Ambient Pressure X-ray Photoelectron Spectroscopy. *J. Phys. Chem. Lett.* **2017**, *8*, 102−108.

(43) Chen, J. Y.; Wanyan, Y. J.; Zeng, J. X.; Fang, H. H.; Li, Z. J.; Dong, Y. D.; Qin, R. X.; Wu, C. Z.; Liu, D. Y.; Wang, M. Z.; et al. Surface Engineering Protocol To Obtain an Atomically Dispersed Pt/CeO₂ Catalyst with High Activity and Stability for CO Oxidation. *ACS Sustainable Chem. Eng.* **2018**, *6*, 14054−14062.

⬚ Recommended by ACS